# Modification of Polyethylene–Octene Elastomer by Silica Through a Sol–Gel Process

**Chin-San Wu, Hsin-Tzu Liao**

*Department of Chemical Engineering, Kao Yuan Institute of Technology, Kaohsiung County, Taiwan 82101, Republic of China*

**ABSTRACT:** In this study, tetraethoxysilane (TEOS) and a metallocene polyethylene–octene elastomer (POE) were chosen as the ceramic precursor and the continuous phase, respectively, for the preparation of new hybrids by an *in situ* sol–gel process. To obtain a better hybrid, a maleic anhydride-grafted polyethylene–octene elastomer (POE-*g*-MAH), used as the continuous phase, was also investigated. Characterizations of POE-*g*-MAH/SiO$_2$ and POE/SiO$_2$ hybrids were performed by Fourier transform infrared (FTIR) and $^{29}$Si solid-state nuclear magnetic resonance (NMR) spectrometers, a differential scanning calorimeter (DSC), a thermogravimetry analyzer, and an Instron mechanical tester. The results showed that the POE-*g*-MAH/SiO$_2$ hybrid could improve the properties of the POE/SiO$_2$ hybrid because the interfacial force between the polymer matrix and the silica network was changed from hydrogen bonds into covalent Si—O—C bonds through dehydration of hydroxy groups in POE-*g*-MAH with residual silanol groups in the silica network. The existence of covalent Si—O—C bonds was proved by FTIR spectra. For the POE/SiO$_2$ and POE-*g*-MAH/SiO$_2$ hybrids, maximum values of the tensile strength and the glass transition temperature were found at 9 wt % SiO$_2$ since a limited content of silica might be linked with the polymer chains through the covalent bond. © 2003 Wiley Periodicals, Inc. J Appl Polym Sci 88: 966–972, 2003

**Key words:** polyolefins; silicas; NMR; DSC

## INTRODUCTION

The synergistic combination of polymers and ceramics via a sol–gel process has recently attracted great attention in the field of material science because it has the potential for the development of new materials with designed properties, by structural manipulation at the molecular level.[1–8] These composite materials join the benefits of polymers (such as flexibility, toughness, and ease processing) with those of ceramics or glasses (such as hardness, durability, and thermal stability). In general, the research of organic–inorganic composite materials has been largely conducted in the inorganic modification of organic polymers, that is, the organic polymer is the dominant phase.[9–11] The polymeric phases, used in ceramic-reinforced polymers by way of a sol–gel process, that have been studied are elastomers such as polydimethylsiloxane and polymethylphenylsiloxane, glassy polymers such as poly(vinyl methacrylate), poly(vinyl acetate), and the ethylene–vinyl acetate copolymer, semicrystalline polymers such as poly(tetramethylene oxide) and polytetrahydrofuron, high-temperature polymers such as aromatic polyamides and polyimides, and other polymeric media such as membranes of perfluorosulfonic acid (Naflon®).[1] The organometallic compounds [M(OC$_n$H$_{2n+1}$)$_z$, where M = Si, Sn, Ti, Zr, Al, etc.] are generally used as the ceramic precursor, and tetraethoxysilane (TEOS) is the most common one. The microstructures and properties of composite materials depend much on the interfacial force between organic and inorganic phases. Formation of a hydrogen or covalent bond between the two phases is normally utilized to establish this interfacial force.[12–14] The formation of a hydrogen bond may have arisen from the basic group of the hydrogen acceptor in the polymer and the hydroxy group of the intermediate species from metal alkoxides. The covalent bond could be formed through dehydration of hydroxy groups in the polymer with residual hydroxy groups in the inorganic network.

Polyethylene is one of the most important thermoplastics but its use was restricted in certain applications by its low melting point, stability in hydrocarbons, and a tendency to crack when stressed. Studies on the graft reaction, crosslinking reaction, and blending with organic fillers for polyethylene, to mitigate its disadvantages, have been extensively undertaken for many years. Recently, the metallocene-based polyethylene–octene elastomer (POE), which was developed using a metallocene catalyst by Dow and Exxon, has received much attention due to its unique uniform distribution of comonomer content and narrow molecular weight distribution.[15,16] A study on the synthe-

sis and characterization of POE/silica hybrids has not been made, although Wang et al.[17] synthesized and characterized maleated polyethylene/clay nanocomposites prepared by simple melt compounding. The purpose of this article was to systematically investigate the properties of the POE/SiO$_2$ and maleic anhydride-grafted polyethylene–octene elastomer (POE-$g$-MAH)/SiO$_2$ hybrids obtained from the sol–gel process. The hybrid products were characterized by Fourier transform infrared (FTIR) spectroscopy and nuclear magnetic resonance (NMR) spectroscopy to understand the structural change between POE/SiO$_2$ and POE-$g$-MAH/SiO$_2$ hybrids. Moreover, a thermogravimetry analyzer (TGA), a differential scanning calorimeter (DSC), and an Instron mechanical tester were also used to examine the thermal stability and mechanical properties of the hybrids.

## EXPERIMENTAL

### Materials

The POE copolymer with 18% octene (Engage 8003) was supplied by the Dow Chemical Corp. (Wilmington, DE). TEOS, maleic anhydride (MAH), and benzoyl peroxide (BPO) were obtained from the Aldrich Chemical Corp. (Milwaukee, WI). Before use, TEOS and MAH were purified by distillation and recrystallization from chloroform, respectively. The free-radical initiator (BPO) was purified by dissolving it in chloroform and reprecipitating with methanol. Other reagents were purified by conventional methods. The POE-$g$-MAH copolymer was made in our laboratory and its grafting percentage was about 1.02 wt %.

### Samples preparation

#### POE-$g$-MAH copolymer

The grafting reaction of MAH onto molten POE was performed using xylene as an interface agent and BPO as an initiator under a nitrogen atmosphere at 85 ± 2°C. The reaction lasted for 6 h with a rotor speed of 60 rpm. The grafting percentage was determined by a titration method[18] and the result showed that it was about 1.02 wt % when BPO and MAH loadings were kept at 0.3 and 10 wt %, respectively.

#### POE/SiO$_2$ and POE-$g$-MAH/SiO$_2$ hybrids

The mixture called "Sol B" was prepared by dissolving a stoichiometric amount of TEOS, H$_2$O, and HCl (as the catalyst) in THF (Table I) and then it was stirred at room temperature for 30 min to obtain a homogeneous solution. According to Table I, a determined amount of POE or POE-$g$-MAH was put into a Brabender "Platograph" 200-Nm mixer W50EHT instrument with a blade-type rotor to melt it under the

**TABLE I**
**Compositions of Various Sol–Gel Liquid Solutions for Preparation of Hybrid Materials**

| Compositions | SiO$_2$ (wt %) | | | | |
| --- | --- | --- | --- | --- | --- |
| | 3 | 6 | 9 | 12 | 20 |
| POE or POE-$g$-MAH (g) | 38.52 | 35.13 | 31.77 | 29.36 | 23.16 |
| TEOS (g) | 4.13 | 7.78 | 10.89 | 13.88 | 20.03 |
| THF (g) | 4.13 | 7.78 | 10.89 | 13.88 | 20.03 |
| Sol B | | | | | |
| [HCl]/[TEOS][a] | 0.01 | 0.01 | 0.01 | 0.01 | 0.01 |
| [H$_2$O]/[TEOS][a] | 2.2 | 2.2 | 2.2 | 2.2 | 2.2 |

[a] The mol ratio of HCl and H$_2$O to TEOS.

conditions that the rotor speed and blending temperature were kept at 50 rpm and 160–170°C, respectively. When the POE or POE-$g$-MAH was melted completely, the Sol B was added to the sol–gel process proceeded for another 10 min. The scheme for the sol–gel process of TEOS and POE-$g$-MAH is summarized in Scheme 1. Prior to characterization, each sample was dried at 150°C in a vacuum oven for 3 days to remove residual solvents. The hybrid products were pressed into a thin plate by a hot press at 140°C and then they were put into a dryer for cooling. Next, the cool thin plate was made into standard specimens for characterization.

### Characterizations of hybrids
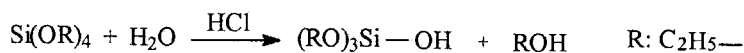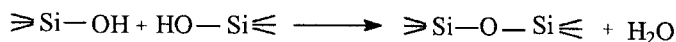
#### FTIR spectral analysis

A Fourier transform infrared transmission spectrophotometer (Bio-Rad FTS-7PC type), using thin films, was used to verify the incorporation of a silicate phase to the extent that Si—O—Si bonds were formed.
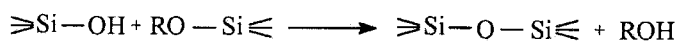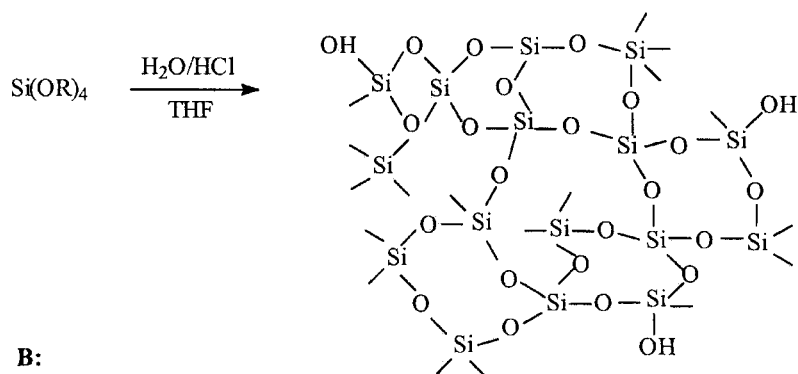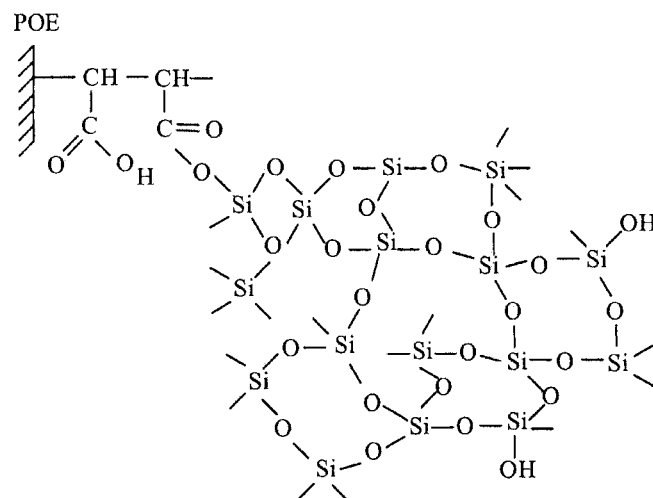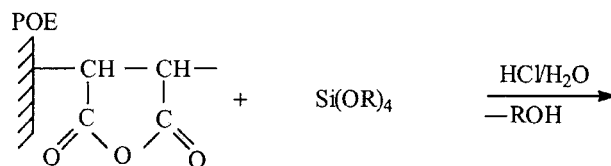
#### $^{29}$Si solid-state NMR analysis

$^{29}$Si-NMR spectra were recorded on a Bruker MSL-400 NMR spectrometer, using a standard double air-bearing cross-polarization/magic angle-spinning probe, operated at a frequency of 79.5 MHz for $^{29}$Si. Samples were loaded into 4-mm fused zirconia and sealed with Kel-F$^{TM}$ caps. Spectra were obtained using the conditions proposed by Siudak et al.[19] but at a spinning rate of ~4700 Hz. The $^{29}$Si solid-state NMR spectra were used to study the degree of molecular connectivity of the silicate phase.

#### TGA/DSC analysis

A thermogravimetry analyzer (TA Instrument 2010 TGA) was used to assess whether organic–inorganic phase interactions influence the thermal degradation of hybrids. Samples were placed in alumina crucibles and tested with a thermal ramp over the temperature range of 30–600°C at a heating rate of 20°C/min and then the initial decomposition temperature (IDT) of

**A: Hydrolysis**

$$Si(OR)_4 + H_2O \xrightarrow{HCl} (RO)_3Si-OH + ROH \qquad R: C_2H_5-$$

**Condensation**

$$\geqslant Si-OH + HO-Si \leqslant \longrightarrow \geqslant Si-O-Si \leqslant + H_2O$$

and/or

$$\geqslant Si-OH + RO-Si \leqslant \longrightarrow \geqslant Si-O-Si \leqslant + ROH$$

**Net Reaction**

$$Si(OR)_4 \xrightarrow[THF]{H_2O/HCl}$$

**B:**

POE + $Si(OR)_4$ $\xrightarrow[-ROH]{HCl/H_2O}$

POE

**Scheme 1**

the hybrid was obtained. The glass transition temperature $(T_g)$ of the samples was determined by a TA Instrument 2010 DSC system. For DSC tests, sample sizes ranged from 4 to 6 mg and the $T_g$ values were obtained from the melting curves taken at a temperature range of $-100$ to $150°C$ and scanned at a rate of $10°C/min$.

Mechanical testing

According to the ASTM D638 method, an Instron mechanical tester (Model LLOYD, LR5K type) was used to measure the tensile strength at break. The films of the testing samples, which were conditioned at $50 \pm 5$ % relative humidity for 24 h prior to the measure-

ments, were prepared in a hydrolytic press at 140°C and then the measurements were done using a 20-mm/min crosshead speed. Five measurements were performed for each sample and the results were averaged to obtain a mean value.

## RESULTS AND DISCUSSION

### Infrared spectroscopy

Figures 1(A–D) show the FTIR spectra of pure POE, POE-*g*-MAH, POE/SiO$_2$, and POE-*g*-MAH/SiO$_2$, respectively. Figure 1 gives the result that all the characteristic peaks of POE at 2840–2928, 1465, and 720 cm$^{-1}$ appear in the four polymers.[20,21] From a comparison between Figure 1(A) and (B), it was found that there are two extra peaks, which are the characteristic peaks of anhydride carbonyl due to the stretching vibration of the —C—O bond at 1781 and 1850 cm$^{-1}$. A similar result can be found in some proposed articles.[20,22] So, one can confirm that MAH was really grafted onto POE since the discernible peaks near 1781 and 1850 cm$^{-1}$, based on free acid, appeared in the spectrum of the modifier POE. From the results of Figure 1(A,C), it can be seen that new peaks at about 3000–3600 cm$^{-1}$ and 400–500 cm$^{-1}$ appear in the FTIR spectrum of the POE/SiO$_2$ composite. The broad O—H bond stretching about 3000–3600 cm$^{-1}$ is due to the formation of OH and hydrogen bonds and the peaks in the 400–500 cm$^{-1}$ indicate the silicate phase. So, one can imply that the interfacial force between the POE matrix and the silica network is only established by the hydrogen bonds.

It can be seen from Figure 1(B,D) that the absorbance for the —C–O stretching vibration in the hydrogen-bonded anhydride group of POE-*g*-MAH is shifted from 1781 and 1850 cm$^{-1}$ to 1709 and 1733 cm$^{-1}$ when the POE-*g*-MAH/SiO$_2$ hybrid is formed. The shift of absorbance for the —C–O stretching vibration is due to the formation of ester and carbonyl groups (Scheme 1).[23] Figure 1(D), compared to the FTIR spectrum of POE-*g*-MAH, also shows that there are four extra peaks at 435, 465, 1086, and 1123 cm$^{-1}$ and an extra broad O—H bond stretching about 3000–3600 cm$^{-1}$. The peaks at 1086 and 1123 cm$^{-1}$ indicate that the Si—C–O bond, which may be associated with an H-bonded Si—OH group, is produced from the reaction between POE-*g*-MAH and SiO$_2$ since absorbance of this covalent bond usually appears at 1080–1200 cm$^{-1}$ (typically at 1080–1120 cm$^{-1}$).[21,23,24] The broad O—H bond stretching at about 3000–3600 cm$^{-1}$ is due to the formation of OH and hydrogen bonds. An interesting trait associated with the silicate phase appears in the limited 500–400-cm$^{-1}$ range for the POE/SiO$_2$ and POE-*g*-MAH/SiO$_2$ hybrids, where it consists of a peak at about 435 cm$^{-1}$ to the right of the peak assigned to Si—O—Si bending deformation at
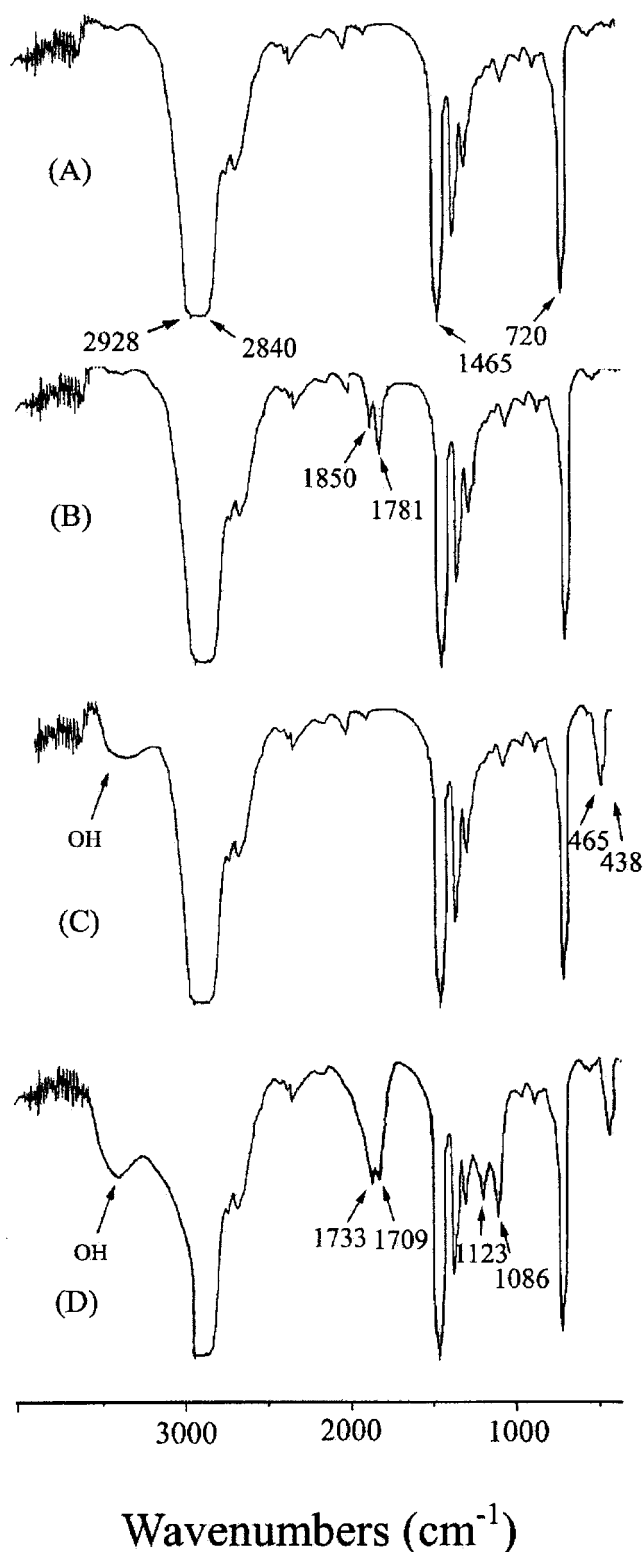


**Figure 1** FTIR spectra of (A) unmodified POE, (B) POE-*g*-MAH, (C) POE/SiO$_2$ (9 wt %), and (D) POE-*g*-MAH/SiO$_2$ (9 wt %).

about 465 cm$^{-1}$. This feature, associated with partially condensed intermediates in the polymerization of TEOS, can be identified as 525 cm$^{-1}$ with Si—(OSi)$_2$
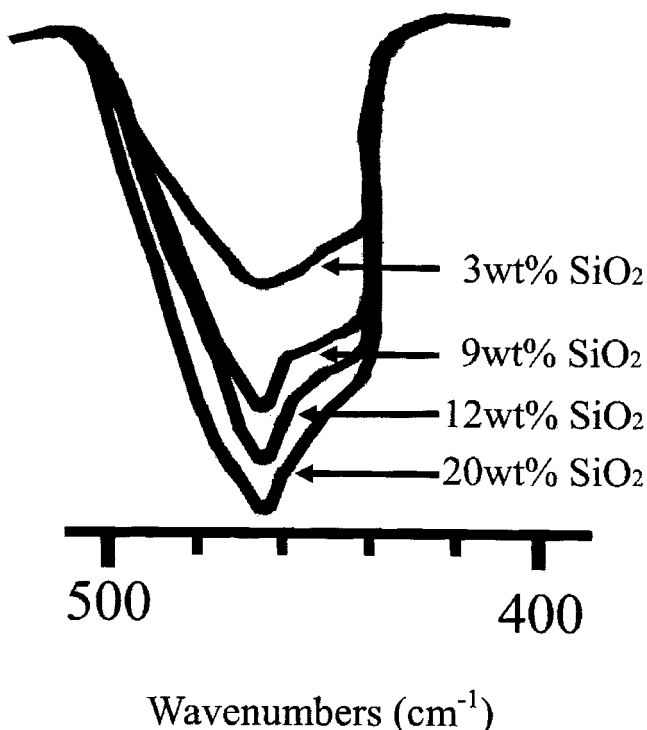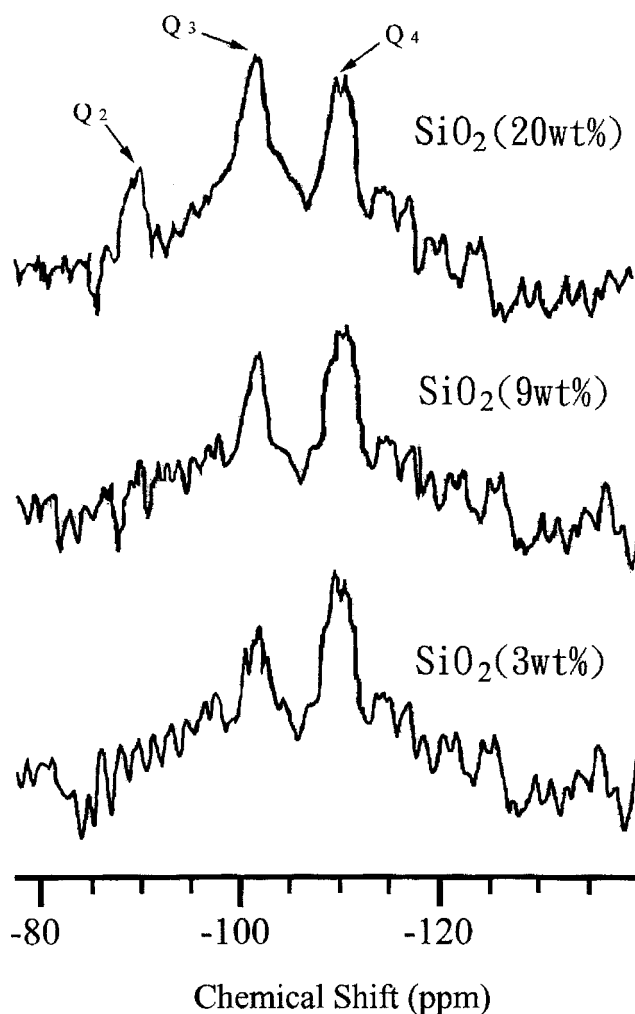
**Figure 2** FTIR spectra of POE-$g$-MAH/SiO$_2$ hybrids with different silica contents in the vicinity of the peak Si—O—Si bending deformation.

species ($^2Q$), 484 cm$^{-1}$ with Si—(OSi)$_3$ species ($^3Q$), and 432 cm$^{-1}$ with Si—(OSi)$_4$ species ($^4Q$).[25] To understand the effect of the silica content on this feature, the spectra in this limited range for POE-$g$-MAH/SiO$_2$ hybrids having different amounts of silica were expanded and are illustrated in Figure 2. Figure 2 shows that the increase in absorbance of the Si—O—Si bending vibration, about 465 cm$^{-1}$, with an increasing silica content is observed since the formation of $^3Q$ is increased. Figure 2 also shows that the relative $^3Q$ through $^4Q$ present in the samples varies with the silica content and it will be studied with $^{29}$Si solid-state NMR and discussed later.

## $^{29}$Si solid-state NMR spectroscopy

The spectra of $^{29}$Si solid-state NMR were used to study the degree of molecular connectivity of the silicate phase. The peak assignments for different degrees of Si atom substitution about the SiO$_4$ tetrahedra were discussed in earlier reports of organic/silica hybrids.[26] Peaks are generally denoted by the symbol $^nQ$ for the Si atom coordination state (RO)$_{4-n}$Si(OSi)$_n$, where R = H or an alkyl group. Each peak is located within a range of chemical shifts relative to Si(Me)$_4$ as follows: $^1Q$ = −68 to −83 ppm, $^2Q$ = −74 to −93 ppm, $^3Q$ = −91 to −101 ppm, and $^4Q$ = −106 to −120 ppm.[19] Figure 3 displays the spectra of POE-$g$-MAH/SiO$_2$ hybrids containing 3, 9, and 20 wt % silica. The chem-

ical-shift distribution consists almost exclusively of $^3Q$ and $^4Q$ species, regardless of the silicate content, although some $^2Q$ character is seen in a higher silicate content (such as >9 wt %). For POE-$g$-MAH/SiO$_2$ hybrids containing 3 and 9 wt %, only peaks $^3Q$ and $^4Q$ can be seen in the spectra and this result might imply that all the silica have reacted with the POE-$g$-MAH copolymer. The appearance of peak $^2Q$ in the spectrum of POE-$g$-MAH/SiO$_2$ (20 wt %) means that an excess amount of silica was introduced to react with the POE-$g$-MAH copolymer since a low value of the grafting percentage may be obtained. It can also be seen in Figure 3 that the intensity of $^3Q$ was increased with an increasing of the silica content but the intensity was decreased slightly for $^4Q$. The considerable degree of $^3Q$ and $^4Q$ coordination states found in the $^{29}$Si solid-state NMR examination is in general agreement with the structural interpretation of the FTIR results and it might infer that some degree of porosity is present since "porous" silicate nanoparticles have a considerable degree of intramolecular disconnection.[19]



**Figure 3** $^{29}$Si solid-state NMR spectra of POE-$g$-MAH/SiO$_2$ hybrids with different silica contents.
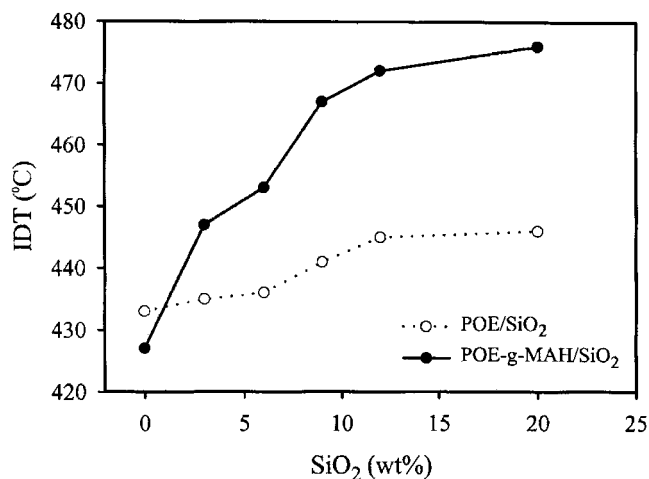
**Figure 4** Curves of initial decomposition temperature versus silica content for POE/SiO$_2$ and POE-$g$-MAH/SiO$_2$ hybrids.

## TGA and DSC tests

The thermal stability of the organic/inorganic hybrid depends on the interaction between the polymer chains and the silica network and the uniform distribution of the silica in the polymer matrix. The effect of the silica content on the value of IDT for the POE/SiO$_2$ and POE-$g$-MAH/SiO$_2$ hybrids is illustrated in Figure 4. It can be seen from Figure 4 that both the POE/SiO$_2$ and POE-$g$-MAH/SiO$_2$ hybrids can have a positive effect on the value of IDT. It is clear that the IDT value of the POE-$g$-MAH/SiO$_2$ hybrid is much higher than that of the POE/SiO$_2$ hybrid, although POE-$g$-MAH lowers the IDT value of POE. However, the IDT value of the POE-$g$-MAH/SiO$_2$ hybrid changed markedly with the silica content, where it increased from 433 to 479°C as the silica content was increased from 3 to 20 wt %. This result is due to that the interfacial force between the polymer chains and silica network is changed from the weaker hydrogen bonding to the stronger covalent Si—C–O bond when POE-$g$-MAH is used to replace POE for the manufacture of the hybrid. For the POE/SiO$_2$ and POE-$g$-MAH/SiO$_2$ hybrids, Figure 4 also shows that the increment in IDT was not significant when the silica content was greater than 9 wt %, since phase separation could occur in the hybrids.

The glass transition temperature ($T_g$) of the POE/SiO$_2$ and POE-$g$-MAH/SiO$_2$ hybrids was obtained from the DSC examination and the result is given in Figure 5. The glass transition temperature of the hybrid composites is associated with a cooperative motion of long-chain segments, which may be hindered by the silica network.[9] So, as shown in Figure 5, both the POE/SiO$_2$ and POE-$g$-MAH/SiO$_2$ hybrids could exhibit a higher value of the glass transition temperature than that of the pure POE. It is also found that the

enhancement in the $T_g$ value for the POE-$g$-MAH/SiO$_2$ hybrids is more significant than that for the POE/SiO$_2$ ones. This indicates that the POE-$g$-MAH/SiO$_2$ hybrids have newly formed covalent Si—C–O bonds, which are stronger than are the hydrogen bonds in hindering the motion of the polymer chains. However, the effect of the silica content on the $T_g$ reveals that both the POE/SiO$_2$ and POE-$g$-MAH/SiO$_2$ hybrids exhibit a maximum value of $T_g$ at 9 wt % SiO$_2$. This phenomenon might be attributed to the presence of excess silica particles, which were only dispersed in the polymer matrix when the silica content was greater than 9 wt %. Such excess particles might cause the separation between the organic and inorganic phases and decrease the compatibility between the silica and POE or POE-$g$-MAH. Therefore, the $T_g$ value of the POE/SiO$_2$ and POE-$g$-MAH/SiO$_2$ hybrids increased with the silica content to a maximum value and then decreased.

## Mechanical tests

Figure 6 shows the variation of the tensile strength at break with the silica content for the POE/SiO$_2$ and POE-$g$-MAH/SiO$_2$ hybrids. The results of Figure 6 show that the POE-$g$-MAH copolymer lowered the tensile strength of POE but the POE-$g$-MAH/SiO$_2$ hybrid enhances the value of the tensile strength significantly. For the POE/SiO$_2$ hybrids, the effect of the silica content on the tensile strength is slight since the interfacial force between the POE chains and the silica network is only the weaker hydrogen bond. With the same silica content, the POE-$g$-MAH/SiO$_2$ hybrid exhibited much better tensile strength than that of the POE/SiO$_2$ one. This obvious enhancement in tensile strength may be attributed to the presence of the silica network and to the formation of a chemical bond,
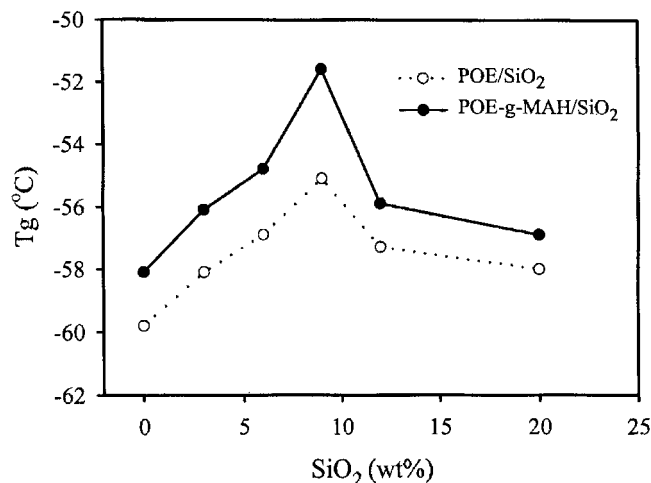


**Figure 5** Curves of glass transition temperature versus silica content for POE/SiO$_2$ and POE-$g$-MAH/SiO$_2$ hybrids.
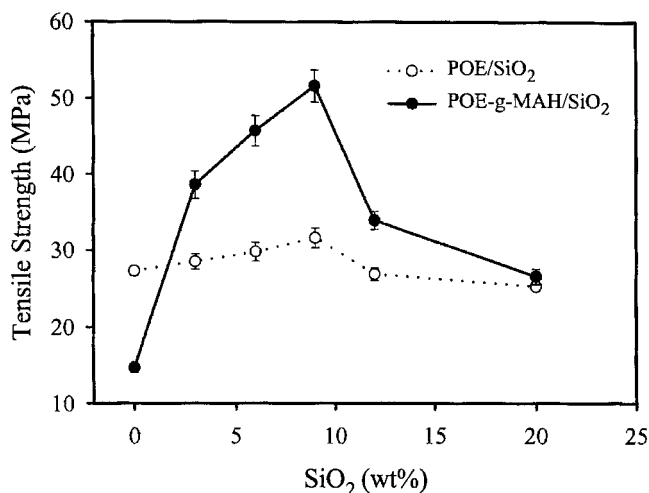
**Figure 6** Curves of tensile strength at break versus silica content for POE/SiO$_2$ and POE-$g$-MAH/SiO$_2$ hybrids.

perhaps the covalent Si—C–O bond hybrid, through the dehydration of the hydroxy group in POE-$g$-MAH with the residual silanol group in the silica network. However, the tensile strength of the POE-$g$-MAH/ SiO$_2$ hybrid increased to 51.6 MPa at 9 wt % silica, but it decreased markedly with the silica content when the concentration of the silica was beyond this point. This phenomenon is also due to that the separation between the organic and inorganic phases occurred in the hybrids having a larger silica content.

## CONCLUSIONS

In this article, organic–inorganic hybrid materials were prepared by an *in situ* sol–gel process of TEOS in the presence of POE or POE-$g$-MAH. The FTIR spectra proved that the MAH was really grafted onto the POE copolymer and the covalent Si—C–O bonds were produced through dehydration of hydroxy groups in POE-$g$-MAH with residual silanol groups in the silica network. $^{29}$Si solid-state NMR spectroscopy was used to probe the degree of molecular connectivity of the silicate phase and the result showed that the Si atom coordination around SiO$_4$ units is predominantly $^3Q$ and $^4Q$. This result is in agreement with the structural interpretation of the FTIR spectra. TGA tests showed that the initial decomposition temperature of the POE-$g$-MAH/SiO$_2$ hybrid was much higher than that of the POE/SiO$_2$ hybrid and pure POE. The trends of the silica content effect on the tensile strength and glass transition temperature are similar. It was found that

there are maximum values of the tensile strength and glass transition temperature at about 9 wt % SiO$_2$ for the POE /SiO$_2$ and POE-$g$-MAH/SiO$_2$ hybrids. This result is because excess silica particles might cause the separation between the organic and inorganic phases and decrease the compatibility between silica and POE or POE-$g$-MAH. Finally, the POE-$g$-MAH/SiO$_2$ hybrids could improve the thermal stability and mechanical properties of the POE/SiO$_2$ hybrids since the interfacial force was changed from hydrogen bonds into covalent Si—C–O bonds through dehydration of hydroxy groups in POE-$g$-MAH with residual silanol groups in the silica network.

## References

1. Mark, J. E. Polym Eng Sci 1996, 36, 2905.
2. Vong, M. S. W.; Bazin, N.; Sermon, P. A. J Sol–Gel Sci Technol 1997, 8, 499.
3. Tamaki, R.; Naka, K.; Chujo, Y. Polym J 1998, 30, 60.
4. Schmidt, H. J Non-Cryst Solids 1985, 73, 681.
5. Ulrich, D. R. J Non-Cryst Solids 1988, 100, 174.
6. Judeinstein, P.; Sanchez, C. J Mater Chem 1996, 6, 511.
7. Huang, H. H.; Orler, B.; Wilkes, G. L. Macromolecules 1987, 20, 1322.
8. Novak, B. M. Adv Mater 1993, 5, 422.
9. Hsu, Y. G.; Chiang, I. J.; Perrier, C.; Lo, J. F. J Appl Polym Sci 2000, 78, 1179.
10. Wilkes, G. L.; Wen, J. In Polymeric Materials Encyclopedia; Salamone, J. C., Ed.; CRC: New York, 1996; Vol. 6, p 2782.
11. Wei, Y.; Yang, D.; Bakthavatchalam, R. Mater Lett 1992, 13, 261.
12. Alsten, J. G. V. Macromolecules 1996, 29, 2163.
13. Fitzgerald, J. J.; Landry, C. J. T.; Pochan, J. M. Macromolecules 1992, 25, 3715.
14. Scherer, G. W. In Ultra-Structure Processing of Advanced Ceramics; Mackenzie, J. D.; Ulrich, D. R., Eds.; Wiley: New York, 1988.
15. Hwang, Y. C.; Chum, S.; Sehanobish, K. ANTEC 1994, 94, 3414.
16. Chum, P. S.; Kao, C. K.; Knight, G. W. Plast Eng 1995, June, 21.
17. Wang, K. H.; Choi, M. H.; Koo, C. M.; Choi, Y. S.; Chung, I. J. Polymer 2001, 42, 9819.
18. Gaylord, N. G.; Mehta, R.; Kumar, V.; Tazi, M. J Appl Polym Sci 1989, 38, 359.
19. Siudak, D. A.; Start, P. R; Mauritz, K. A. J Appl Polym Sci 2000, 77, 2832.
20. Chandra, R.; Rustgi, R. Polym Degrad Stab 1997, 56, 185.
21. Breslin, V. T.; Li, B. J Appl Polym Sci 1993, 48, 2063.
22. Yu, Z. Z.; Ou, Y. C.; Qi, Z. N.; Hu, G. H. J Polym Sci Part B Polym Phys 1998, 36, 1987.
23. Landry, C. J. D.; Coltrain, B. K.; Wesson, J. A.; Zumbulyadis, N.; Lippert, J. L. Polymer 1992, 33, 1496.
24. Zhou, W.; Dong, J. H.; Qiu, K. Y.; Wei, Y. J Appl Polym Sci 1998, 36, 1607.
25. Lippert, J. L.; Melpolder, S. M.; Kelts, L. M. J Non-Cryst Solids 1988, 104, 139.
26. Siudak, D. A.; Mauritz, K. A. J Polym Sci Part B Polym Phys 1999, 37, 143.